

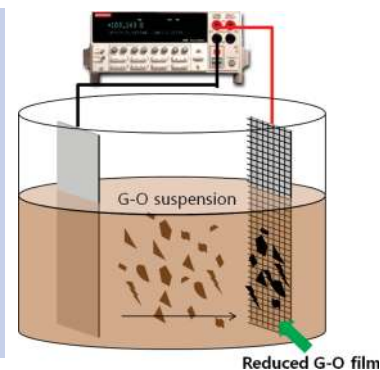
Thin Film Fabrication and Simultaneous Anodic Reduction of Deposited Graphene Oxide Platelets by Electrophoretic Deposition

Sung Jin An,[†] Yanwu Zhu,[†] Sun Hwa Lee,[†] Meryl D. Stoller,[†] Tryggvi Emilsson,[§] Sungjin Park,[†] Aruna Velamakanni,[†] Jinho An,[†] and Rodney S. Ruoff*^{·†}

[†]Department of Mechanical Engineering and the Texas Materials Institute, The University of Texas at Austin, One University Station C2200, Austin, Texas, 78712-0292, [‡]Department of Materials Science and Engineering, KAIST, 373-1, Guseong-dong, Yuseong-gu, Daejeon, 305-701 Korea, and [§]APL Engineered Materials, Inc., 2401 North Willow Road, Urbana, Illinois, 61802

ABSTRACT We report the deposition of films composed of overlapped and stacked platelets of graphene oxide (G-O) reduced by an electrophoretic deposition (EPD) process. The oxygen functional groups of G-O were significantly removed by the EPD process, and the as-deposited G-O film by EPD showed improved electrical conductivity ($1.43 \times 10^4 \text{ S} \cdot \text{m}^{-1}$) over G-O papers made by the filtration method ($0.53 \times 10^{-3} \text{ S} \cdot \text{m}^{-1}$). This method for reducing G-O without added reducing agents has the potential for high-yield, large-area, low-cost, and environmentally friendly production of films composed of reduced G-O platelets.

SECTION Nanoparticles and Nanostructures



Considerable research has been recently devoted to graphene-based materials because of their excellent electrical, mechanical, and thermal properties, and their possibilities for applications as transparent conductive film, in composite materials, and others.^{1–9} In particular, recent achievements in homogeneous colloidal suspensions of chemically reduced graphene oxide (G-O) platelets in various organic solvent systems have drawn particularly high interest as a result of the possibility for low-cost and high-volume production, as well as the flexibility of use of a wide range of solvent-based manufacturing processes.^{4,10,11} Chemically reduced G-O has already been used to show proof of concept in fabricating field effect transistors (FETs), single-molecule gas detectors, ultracapacitors, solar cells, liquid crystal devices, transparent conducting films, polymer composites, and so forth.^{1,2,11–19} Solution-based deposition methods, including membrane filtration,^{2,20} dip coating,¹⁶ layer-by-layer (LbL),^{21,22} spray-coating,²³ and spin coating^{12,24} have been reported for preparing graphene-based material thin films. The size of films from the time-consuming membrane filtration method is limited by the size of the membrane, and thus the method is not suitable for large area production of graphene-based thin films. While dip coating, LbL, spin coating, and spray-coating methods can be used to directly deposit graphene-based material on large area substrates, it is difficult to control the thickness and uniformity of the graphene-based material as a thin film.²⁵ There is thus a need for control of uniformity and thickness for large area thin films.

The electrophoretic deposition (EPD) method is a well-developed and economical method that has been successfully applied for the deposition of carbon nanotubes and thermally expanded graphite oxide (GO) particles for transparent

conducting films and phosphors for display.^{26–28} In particular, the EPD method has a number of advantages in the preparation of thin films from charged colloidal suspensions, such as high deposition rate, good thickness controllability, good uniformity, and simplicity of scale up. Here, we demonstrate that the EPD method can be utilized to deposit films of graphene. Interestingly, we observed that the as-deposited G-O film by EPD (EPD-gO films) made by this approach had significantly lower oxygen content as a result of the EPD process. Reduction of G-O has typically been done with chemical agents such as hydrazine^{4,29} and/or strong alkaline solutions (NaOH/KOH),³⁰ or requires moderately high temperature treatments.³¹ Low-temperature and/or methods free of harsh chemicals for reducing the oxygen content of G-O are relevant for achieving high-yield, low-cost, and environmentally friendly production of “reduced G-O”.

The GO used in this study was synthesized from purified natural graphite by the modified Hummers method.³² GO was dispersed in water and sonicated for 2 h at room temperature. After the preparation of colloidal suspensions of individual G-O platelets in purified water, EPD-gO was deposited by EPD on 200 mesh stainless steel, and on various other electrically conductive substrates. Typical concentrations of G-O and applied direct current (DC) voltage were 1.5 mg/mL and 10 V, respectively. The deposition time was in the range of 1–10 min. Figure 1a shows a diagram of the single-compartment EPD cell experiment.

Received Date: January 20, 2010

Accepted Date: March 9, 2010

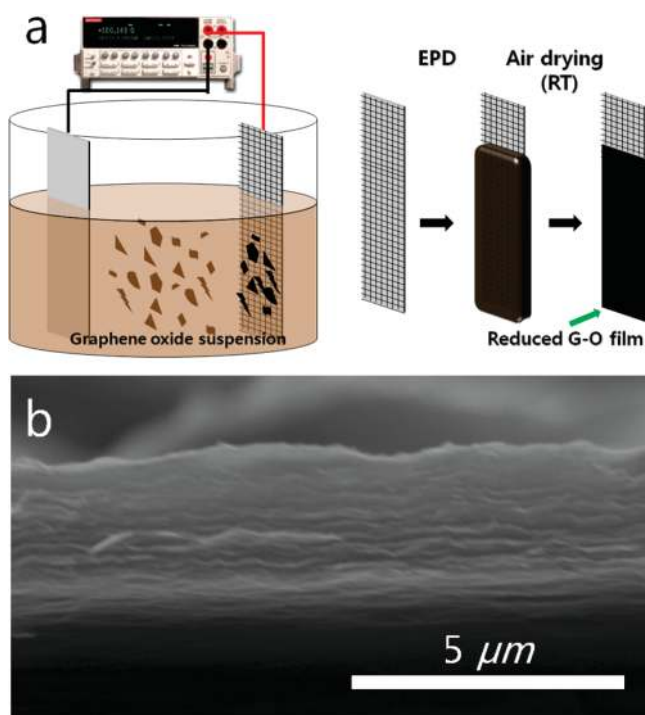


Figure 1. (a) Schematic diagram of the EPD process and (b) cross-sectional SEM image of EPD-gO film.

The G-O platelets migrated toward the positive electrode when a DC voltage was applied. The deposition rate depended on several experimental factors including the concentration of the G-O suspension, the applied DC voltage, and the conductivity of the substrate. We deposited EPD-gO films on various substrates including Cu, Ni, Al, stainless steel, and p-type Si. When an EPD-gO film was deposited on a heavily p-type-doped Si substrate under otherwise identical experimental conditions, the deposition time increased about 5-fold compared to the stainless steel substrate for the same thickness of deposited materials. The stainless steel substrates were used in this experiment to suppress the formation of metal hydroxides at the electrode.^{26,33} During EPD, evolution of gas bubbles at the cathode was observed, and the deposition took place on the anode. When a 1.5 mg/mL G-O suspension was used, a smooth film was deposited on the stainless steel positive electrode in less than 30 s with 10 V of applied potential. After deposition, samples were air-dried at room temperature for 24 h. Figure 1b shows a cross-sectional scanning electron microscopy (SEM) image of an air-dried EPD-gO film with a 4- μm thickness that was deposited in 2 min. (Supporting Information, SFigure 2) The film thickness was uniform, and the packing morphology of the EPD-gO film is similar to G-O paper-like materials formed by filtration.⁴ By varying the current and time, films with thicknesses in the range between several hundreds of nanometers and tens of micrometers could be deposited. As long as the substrate is conducting, a uniform homogeneous film could be deposited.

Raman spectroscopy was used to analyze the EPD-gO film. As shown in Figure 2, the Raman spectrum of the EPD-gO film shows a D-band around 1350 cm^{-1} , a G-band around

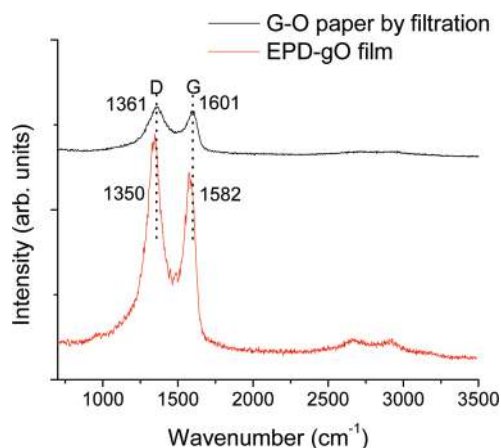


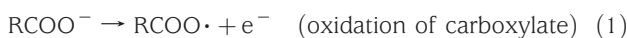
Figure 2. Raman spectra of G-O paper by filtration (black) and EPD-gO film (red).

1582 cm^{-1} , and a broad 2D-band around 2800 cm^{-1} .²⁹ The D-band was detected at 1350 cm^{-1} , which is due to defects or edges.³⁴ The D-, G-, and 2D-bands are shifted to lower wave numbers for the EPD-gO film as compared to G-O paper obtained by filtration. For example, the G-band is at 1601 cm^{-1} for G-O paper made by filtration, but is at 1582 cm^{-1} for the EPD-gO film. The shift to lower wavenumber of the G-band peak of the EPD-gO film presumably results from the reduction of G-O platelets comprising the EPD-gO film.³⁵

The interlayer spacing of the overlapped and stacked platelets comprising the EPD-gO film was investigated by X-ray diffraction (XRD) measurements (see Supporting Information for XRD data). The XRD of air-dried EPD-gO film shows a broad diffraction peak observed at a 2θ value of 18°. The mean interlayer spacing calculated from the 2θ value at the peak maxima of the EPD-gO film was approximately 5.1 Å, which is larger than the d_{002} -spacing of graphite (3.35 Å) and much smaller than the interlayer spacing of G-O paper (8.0–8.3 Å, measured in ambient, approximately 45% relative humidity).^{2,10,36} On the other hand, the XRD spectrum of 100 °C annealed EPD-gO film was shifted to around 24° (3.70 Å), which is slightly larger than the d_{002} -spacing of graphite. The reason for the reduction of interplatelet spacing of EPD-gO film as compared to the interlayer spacing of G-O paper can be attributed to the fact that the water molecules trapped between the hydrophilic G-O platelets in the G-O paper samples obtained by filtration are negligible in the film obtained by EPD.¹⁰

The electrical conductivity of the air-dried EPD-gO as measured by the van der Pauw method was found to be $10.34 \times 10^2 \text{ S}\cdot\text{m}^{-1}$. This value is significantly higher than that of the insulating G-O paper obtained by the filtration method ($0.53 \times 10^{-3} \text{ S}\cdot\text{m}^{-1}$).²⁰ Furthermore, the conductivity of these EPD-gO films after annealing in air at 100 °C for 60 min was $1.43 \times 10^4 \text{ S}\cdot\text{m}^{-1}$. Elemental analysis shows an increase in the C/O atomic ratio of air-dried EPD-gO film (6.2:1) compared to G-O paper obtained by the filtration method (1.2:1, this value includes the contribution of trapped interlamellar water).²⁰ In addition, the C/O atomic ratio of EPD-gO film after annealing at 100 °C was 9.3:1. On the basis

of the comparison of the C/O atomic ratio of the G-O film with chemically reduced G-O by hydrazine ("CReGO"; 10.3:1),²⁹ the EPD-gO film obtained here seems to have a higher O atom concentration than the CReGO, but much less than G-O paper obtained by the simple filtration method. This indicates that deoxygenation is occurring during the EPD process—but at the anode. This seems counterintuitive because oxidation occurs at the anode in an electrolysis cell. The possible electrochemical reactions could be



The GO produced by the Hummers method has oxygen-based functional groups such as hydroxyl and epoxide on the basal planes, and carboxylate and carbonyl functional groups at the edges.⁴ Therefore, the oxygen functional groups (some fraction of them) on exfoliated GO, i.e., G-O platelets, presumably can be removed by and during the EPD process. The reaction scheme above is similar to the Kolbe reaction.³⁷ The GO platelets are negatively charged, due to the abundant deprotonated carboxylate groups, and are thus electrophoretically drawn to the positive electrode. No electrochemical reactions occur (Kolbe, or otherwise), until electronic contact to the anode is made. Once electronic contact to the anode is made, electrons can move away from the platelets, causing oxidation of many of the carboxylate groups on the periphery of the platelets. All of the unpaired electrons formed by the Kolbe-like loss of CO₂ are then free to migrate through the G-O framework, to find other unpaired electrons and form covalent bonds. The reaction of radicals to form two-electron bonds occurs mostly within the graphene platelets. However, formation of bonds between platelets that are close enough and favorably oriented could also happen. A few such bonds, however, would probably not be significant since they would be unlikely to lead to large-scale conjugation of the two platelets of aromatic carbons. This Kolbe-like decarboxylation may explain the loss of carboxylates, but it does not address the loss of epoxide oxygen atoms. We do not know whether they are lost in the form of O₂, H₂O, H₂O₂, CO, CO₂, or some organic molecule(s). Sampling any evolved gases with a mass spectrometer might identify any volatile fragments. An ion selective electrode could monitor evolved carbonate. Electrochemical measurements (e.g., coulometry and voltammetry) along with elemental analysis of the deposited films might also shed light on the mass balance of the reactions involved.

X-ray photoelectron spectroscopy (XPS) was used to evaluate the surface layers of the EPD-gO films. As shown in Figure 3, the C1s spectrum of G-O paper obtained by filtration shows two dominant peaks centered at 284.6 and 286.7 eV with a weak peak at 288.7 eV. As for the origins of the C1s peaks, the peak at 284.6 eV is associated with the binding energy of sp² C–C bonds. The peak at 286.7 eV corresponds to C–O bonds in the epoxy/ether groups.^{29,38} Additionally, the peak around 288.7 eV is assigned as C=O bonds in ketone/carboxylic groups.³¹ In comparison to the C1s spectrum of

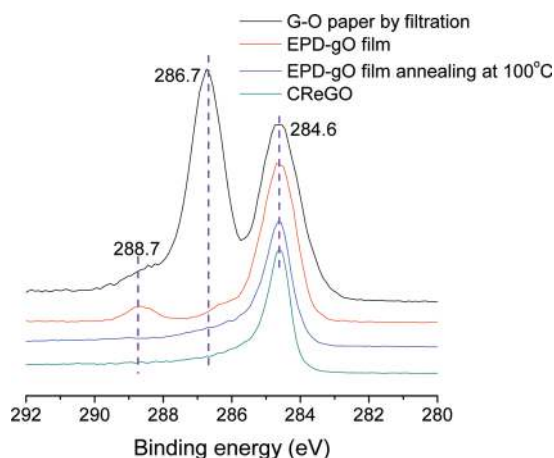


Figure 3. XPS spectra of G-O paper by filtration (black), EPD-gO film (red), EPD-gO film after annealing at 100 °C (blue), and CReGO (green).

the G-O paper obtained by the filtration method, that of the EPD-gO film showed suppression of the epoxy/ether groups (286.7 eV) peak while a small peak at 288.7 eV remains. However, after annealing at 100 °C in air, the oxygen-containing functional group peaks almost disappear, and the peak shape becomes similar to that of CReGO that was obtained by reduction of G-O with hydrazine.²⁹

Also, thermal gravimetric analysis (TGA) of EPD-gO film showed a weight loss of ~8 wt % around 100 °C,^{12,20} likely due to evaporation of water molecules that were contained in the material (see Supporting Information). Such removal of water by heating at 100 °C is supported by the aforementioned XRD. It is known from other work that significant deoxygenation of GO and also of G-O does not occur until temperatures of roughly 200 °C. Of course, the processes are a kinetic one, so the exposure time matters, and "reduction" by evolution of carbon monoxide/carbon dioxide can occur at lower temperatures given sufficient time, but the "lower temperature" is around 150 °C or so unless the time is very long. It, thus, is fair to say that the platelets in the EPD-gO film have a C:O ratio of about 9:1, with the balance of additional oxygen from the elemental analysis value of 6:1 (i.e., prior to heating at 100 °C), arising from interlamellar water that is by and large removed by heating at 100 °C. Therefore, heat treatment at 100 °C partially removes the oxygen functional groups on the G-O platelets and fully removes the water from the paper-like G-O material. Furthermore, the Fourier transform infrared spectroscopy (FT-IR) spectrum of the deposited EPD-gO film shows a significant decrease in the intensity of the peaks related to oxygen functional groups (Figure 4). This shows, along with the chemical analysis by XPS and elemental analysis by the combustion method and the relatively small interlayer spacing by XRD, that the EPD-gO film was significantly reduced during the EPD process.

In summary, we have demonstrated the successful deposition of films composed of overlapped and stacked platelets of reduced G-O by an EPD process. The oxygen functional groups of G-O were significantly removed by the EPD process and the as-deposited EPD-gO film showed improved electrical

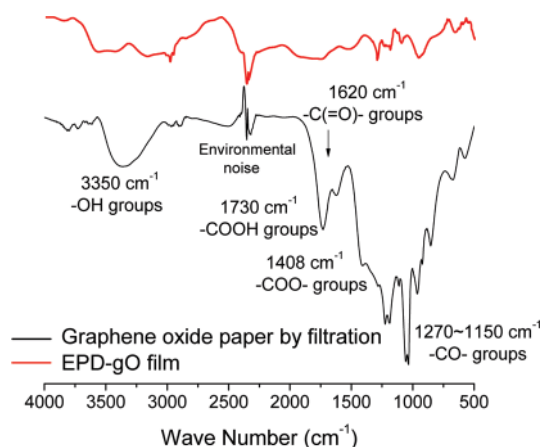


Figure 4. FT-IR spectra of G-O paper by filtration (black) and EPD-gO film (red).

conductivity over G-O papers made by the filtration method. Also, there is essentially no adhesion after the as-deposited film dries. Thus, this method for reducing G-O without harsh and toxic chemicals, and at room temperature, has the potential for rapid, high-yield, large-area, low-cost, and environmentally friendly production of films composed of paper-like samples that are easily removed from the anode. This approach should find utility in a variety of applications including facile coating of complex surfaces and shapes.

SUPPORTING INFORMATION AVAILABLE Experimental details and supporting figures. This material is available free of charge via the Internet at <http://pubs.acs.org>.

AUTHOR INFORMATION

Corresponding Author:

*To whom correspondence should be addressed. E-mail: r.ruoff@mail.utexas.edu

ACKNOWLEDGMENT S.J.A. was partially supported by a Korea Research Foundation Grant funded by the Korean Government (KRF-2008-357-D00113). We thank Dr. Fu-Ren F. Fan and Prof. Allen J. Bard for helpful discussion. Support from the University of Texas in terms of startup funds to R.S.R. is appreciated, as well as support from Graphene Energy, Inc., and by the U.S. Department of Energy, Office of Basic Energy Sciences, Division of Materials Sciences and Engineering under Award DE-SC001951.

REFERENCES

- (1) Stankovich, S.; Dikin, D. A.; Dommett, G. H. B.; Kohlhaas, K. M.; Zimney, E. J.; Stach, E. A.; Piner, R. D.; Nguyen, S. B. T.; Ruoff, R. S. Graphene-Based Composite Materials. *Nature* **2006**, *442*, 282–286.
- (2) Dikin, D. A.; Stankovich, S.; Zimney, E. J.; Piner, R. D.; Dommett, G. H. B.; Evmenenko, G.; Nguyen, S. B. T.; Ruoff, R. S. Preparation and Characterization of Graphene Oxide Paper. *Nature* **2007**, *448*, 457–460.
- (3) Li, X.; Cai, W.; An, J.; Kim, S.; Nah, J.; Yang, D.; Piner, R.; Velamakanni, A.; Jung, I.; Tutuc, E. Large-Area Synthesis of

High-Quality and Uniform Graphene Films on Copper Foils. *Science* **2009**, *324*, 1312–1314.

- (4) Park, S.; Ruoff, R. S. Chemical Methods for the Production of Graphenes. *Nat. Nanotechnol.* **2009**, *4*, 217–224.
- (5) Novoselov, K. S.; Geim, A. K.; Morozov, S. V.; Jiang, D.; Zhang, Y.; Dubonos, S. V.; Grigorieva, I. V.; Firsov, A. A. Electric Field Effect in Atomically Thin Carbon Films. *Science* **2004**, *306*, 666–669.
- (6) Geim, A. K.; Novoselov, K. S. The Rise of Graphene. *Nat. Mater.* **2007**, *6*, 183–191.
- (7) Wu, J.; Pisula, W.; Mullen, K. Graphenes as Potential Material for Electronics. *Chem. Rev.* **2007**, *107*, 718–747.
- (8) Zhang, Y.; Tan, Y. W.; Stormer, H. L.; Kim, P. Experimental Observation of the Quantum Hall Effect and Berry's Phase in Graphene. *Nature* **2005**, *438*, 201–204.
- (9) Balandin, A. A.; Ghosh, S.; Bao, W.; Calizo, I.; Teweldebrhan, D.; Miao, F.; Lau, C. N. Superior Thermal Conductivity of Single-Layer Graphene. *Nano Lett.* **2008**, *8*, 902–907.
- (10) Park, S.; An, J.; Jung, I.; Piner, R. D.; An, S. J.; Li, X.; Velamakanni, A.; Ruoff, R. S. Colloidal Suspensions of Highly Reduced Graphene Oxide in a Wide Variety of Organic Solvents. *Nano Lett.* **2009**, *9*, 1593–1597.
- (11) Li, X.; Wang, X.; Zhang, L.; Lee, S.; Dai, H. Chemically Derived, Ultrasmooth Graphene Nanoribbon Semiconductors. *Science* **2008**, *319*, 1229–1232.
- (12) Tung, V. C.; Allen, M. J.; Yang, Y.; Kaner, R. B. High-Throughput Solution Processing of Large-Scale Graphene. *Nat. Nanotechnol.* **2008**, *4*, 25–29.
- (13) Robinson, J. T.; Perkins, F. K.; Snow, E. S.; Wei, Z.; Sheehan, P. E. Reduced Graphene Oxide Molecular Sensors. *Nano Lett.* **2008**, *8*, 3137–3140.
- (14) Stoller, M. D.; Park, S.; Zhu, Y.; An, J.; Ruoff, R. S. Graphene-Based Ultracapacitors. *Nano Lett.* **2008**, *8*, 3498–3502.
- (15) Wu, J.; Becerril, H. A.; Bao, Z.; Liu, Z.; Chen, Y.; Peumans, P. Organic Solar Cells with Solution-Processed Graphene Transparent Electrodes. *Appl. Phys. Lett.* **2008**, *92*, 263302.
- (16) Wang, X.; Zhi, L.; Mullen, K. Transparent, Conductive Graphene Electrodes for Dye-Sensitized Solar Cells. *Nano Lett.* **2008**, *8*, 323–327.
- (17) Blake, P.; Brimicombe, P. D.; Nair, R. R.; Booth, T. J.; Jiang, D.; Schedin, F.; Ponomarenko, L. A.; Morozov, S. V.; Gleeson, H. F.; Hill, E. W. Graphene-Based Liquid Crystal Device. *Nano Lett.* **2008**, *8*, 1704–1708.
- (18) Eda, G.; Fanchini, G.; Chhowalla, M. Large-Area Ultrathin Films of Reduced Graphene Oxide As a Transparent and Flexible Electronic Material. *Nat. Nanotechnol.* **2008**, *3*, 270–274.
- (19) Watcharotone, S.; Dikin, D. A.; Stankovich, S.; Piner, R.; Jung, I.; Dommett, G. H. B.; Evmenenko, G.; Wu, S. E.; Chen, S. F.; Liu, C. P. Graphene–Silica Composite Thin Films As Transparent Conductors. *Nano Lett.* **2007**, *7*, 1888–1892.
- (20) Park, S.; An, J.; Piner, R. D.; Jung, I.; Yang, D.; Velamakanni, A.; Nguyen, S. B. T.; Ruoff, R. S. Aqueous Suspension and Characterization of Chemically Modified Graphene Sheets. *Chem. Mater.* **2008**, *20*, 6592–6594.
- (21) Li, X.; Zhang, G.; Bai, X.; Sun, X.; Wang, X.; Wang, E.; Dai, H. Highly Conducting Graphene Sheets and Langmuir–Blodgett Films. *Nat. Nanotechnol.* **2008**, *3*, 538–542.
- (22) Cote, L. J.; Kim, F.; Huang, J. Langmuir–Blodgett Assembly of Graphite Oxide Single Layers. *J. Am. Chem. Soc.* **2009**, *131*, 1043–1049.
- (23) Gilje, S.; Han, S.; Wang, M.; Wang, K. L.; Kaner, R. B. A Chemical Route to Graphene for Device Applications. *Nano Lett.* **2007**, *7*, 3394–3398.

- (24) Tung, V. C.; Chen, L. M.; Allen, M. J.; Wassei, J. K.; Nelson, K.; Kaner, R. B.; Yang, Y. Low-Temperature Solution Processing of Graphene–Carbon Nanotube Hybrid Materials for High-Performance Transparent Conductors. *Nano Lett.* **2009**, *9*, 1949–1955.
- (25) Vozar, S.; Poh, Y.; Serbowicz, T.; Bachner, M.; Podsiadlo, P.; Qin, M.; Verploegen, E.; Kotov, N.; Hart, A. Automated Spin-Assisted Layer-by-Layer Assembly of Nanocomposites. *Rev. Sci. Instrum.* **2009**, *80*, 023903.
- (26) Van der Biest, O. O.; Vandeperre, L. J. Electrophoretic Deposition of Materials. *Annu. Rev. Mater. Sci.* **1999**, *29*, 327–352.
- (27) Pei, S.; Du, J.; Zeng, Y.; Liu, C.; Cheng, H. M. The Fabrication of a Carbon Nanotube Transparent Conductive Film by Electrophoretic Deposition and Hot-Pressing Transfer. *Nanotechnology* **2009**, *20*, 235707.
- (28) Hong, S.; Jung, S.; Kang, S.; Kim, Y.; Chen, X.; Stankovich, S.; Ruoff, S. R.; Baik, S. Dielectrophoretic Deposition of Graphite Oxide Soot Particles. *J. Nanosci. Nanotechnol.* **2008**, *8*, 424–427.
- (29) Stankovich, S.; Dikin, D. A.; Piner, R. D.; Kohlhaas, K. A.; Kleinhammes, A.; Jia, Y.; Wu, Y.; Nguyen, S. B. T.; Ruoff, R. S. Synthesis of Graphene-Based Nanosheets via Chemical Reduction of Exfoliated Graphite Oxide. *Carbon* **2007**, *45*, 1558–1565.
- (30) Fan, X.; Peng, W.; Li, Y.; Li, X.; Wang, S.; Zhang, G.; Zhang, F. Deoxygenation of Exfoliated Graphite Oxide under Alkaline Conditions: A Green Route to Graphene Preparation. *Adv. Mater.* **2008**, *20*, 4490–4493.
- (31) Yang, D.; Velamakanni, A.; Bozoklu, G.; Park, S.; Stoller, M.; Piner, R. D.; Stankovich, S.; Jung, I.; Field, D. A.; Ventrice, C. A. Chemical Analysis of Graphene Oxide Films after Heat and Chemical Treatments by X-ray Photoelectron and Micro-Raman Spectroscopy. *Carbon* **2009**, *47*, 145–152.
- (32) Hummers, W. S., Jr.; Offeman, R. E. Preparation of Graphitic Oxide. *J. Am. Chem. Soc.* **1958**, *80*, 1339–1339.
- (33) Thomas, B. J. C.; Boccaccini, A. R.; Shaffer, M. S. P. Multi-walled Carbon Nanotube Coatings Using Electrophoretic Deposition (EPD). *J. Am. Ceram. Soc.* **2005**, *88*, 980–982.
- (34) Casiraghi, C.; Hartschuh, A.; Qian, H.; Piscanec, S.; Georgi, C.; Fasoli, A.; Novoselov, K.; Basko, D.; Ferrari, A. Raman Spectroscopy of Graphene Edges. *Nano Lett.* **2009**, *9*, 1433–1441.
- (35) Ramesha, G. K.; Sampath, S. Electrochemical Reduction of Oriented Graphene Oxide Films: An In Situ Raman Spectroelectrochemical Study. *J. Phys. Chem. C* **2009**, *113*, 7985–7989.
- (36) Buchsteiner, A.; Lerf, A.; Piepers, J. Water Dynamics in Graphite Oxide Investigated with Neutron Scattering. *J. Phys. Chem. B* **2006**, *110*, 22328–22338.
- (37) Vijn, A. K.; Conway, B. E. Electrode Kinetic Aspects of the Kolbe Reaction. *Chem. Rev.* **1967**, *67*, 623–664.
- (38) John, F. M.; William, F. S.; Peter, E. S.; Kenneth, D. B. *Handbook of X-ray Photoelectron Spectroscopy*; Physical Electronics: Eden Prairie, MN, 1995.